Heliyon 10 (2024) e25876

Contents lists available at ScienceDirect

Heliyon

journal homepage: www.cell.com/heliyon

Research article

Image analyses of artificially damaged carbon/glass/ epoxy composites before and after impact load

Burak Öztaş [a,*], Yasemin Korkmaz [a], Halil İbrahim Çelik [b]

[a] Department of Textile Engineering, Kahramanmaraş Sütçü İmam University, Kahramanmaraş, Turkey
[b] Department of Textile Engineering, Gaziantep University, Gaziantep, Turkey

ARTICLE INFO

Keywords:
Artificial damage with glass lamella
Ultrasonic nondestructive testing
Through transmission method (TTU)
Image processing
Damage analysis
Drop-weight impact analysis

ABSTRACT

In recent years, there has been a widespread utilization of composite materials, particularly in critical sectors such as aircraft manufacturing, where errors can have significant consequences. This has generated a need for effective protection of composite materials both during and after production. Detecting internal damage in composite materials, which is often visually imperceptible, becomes crucial and can be assessed using non-destructive testing methods. In this study, glass and carbon woven fabric-reinforced epoxy composites intentionally embedded with artificial damages during manufacturing were subjected to impact tests. The composite materials were scanned using the ultrasonic method to detect damages before and after the impacts. Particularly in glass fiber-reinforced composites (GFRP), the damaged area in the artificially damaged glass lamella sample (G/AL) was calculated to be 4–5 times higher than in the undamaged sample (G/UD). Damaged area values in GFRP were calculated as 72.88 mm^2 in the G/UD sample, 143.74 mm^2 in the G/AC sample, and 315.93 mm^2 in the G/AL sample. While the samples with artificial damage in carbon fiber-reinforced composites (C/AL, C/AC) were perforated during the impact tests, the undamaged samples (C/UD) were not. The images obtained were evaluated using image processing algorithms and were employed in damage analysis. In conclusion, the applied method and the developed image processing algorithm yielded successful results in analyzing barely visible damages and detecting damaged areas.

1. Introduction

Fiber-reinforced composites are widely used in the sports, automotive, and aerospace industries due to their higher specific strength, specific stiffness, and lighter weight compared to metal materials [1–5]. These materials, which are produced with high-performance expectations, may experience many types of damages due to the effects they are exposed to during use or the disruptions in the production process. Even minor damages can have a significant impact on the durability of composite materials [6]. Damage types, such as delamination and cracks in composite materials, not only compromise the stability and strength of the structure over time but also diminish safety performance during application. In these structures, complex damage mechanisms occur that are not observed in metal materials, including fiber breakage, separation from the interface, or delamination [7,8]. Some damages carry a significant risk owing to critical strength loss in the part of the material that is not visible from the outside, called Barely Visible Impact Damage (BVID) [9–13]. These damages are difficult to detect due to the different modes of damage that fiber-reinforced composites

* Corresponding author.
E-mail address: burakoztas@ksu.edu.tr (B. Öztaş).

https://doi.org/10.1016/j.heliyon.2024.e25876
Received 30 May 2023; Received in revised form 4 February 2024; Accepted 5 February 2024
Available online 10 February 2024

exhibit from conventional materials [14].

There are many destructive and non-destructive testing methods for damage analysis in composite materials. Non-destructive tests are the general name of the test methods performed without damaging the integrity of the material. Non-destructive testing methods have been widely used in many fields for a long time among which "Ultrasonic Testing" is the most preferred method [15]. Ultrasonic test methods have been widely used in damage detection studies on fiber-reinforced composite materials [16–20]. Priya and Vinayagam [21], in their study on damage analysis of E-Glass/epoxy composites, stated that the ultrasonic c-scan method can be used as an effective and reliable tool to measure and evaluate the extent of damage. Kostopoulos [22] et al. used the ultrasonic c-scanning method to image damage healing in carbon/epoxy composites and obtained successful results. In their study, Jakubczak and Bienias [23] investigated the possibilities of applying ultrasonic testing in the evaluation of fiber metal composite laminates (FML). The ultrasonic c-scan method has proven effective in assessing the condition of hybrid laminates.

With the development of digital systems, highly capable systems have been developed for the creation, analysis, and processing of images obtained from image capture detectors and elements through computer systems adapted to many fields [24]. The processing of the signals obtained by this method with image processing techniques is necessary to make the data suitable for the improvement of pictorial information and to make autonomous machine detection more convenient by processing the image data for storage and transmission [25]. In a study by Hasiotis, carbon/epoxy and glass/epoxy samples, in which artificial damage layers of different sizes were placed, were examined according to the ultrasonic imaging method. The result of which was that clear images from carbon/epoxy samples could be obtained but not from glass/epoxy samples [16]. Similarly, Hassen et al. [26]in their study on the detection of artificial damages placed in glass-fiber/polypropylene (PP) thermoplastic composite by the ultrasonic testing method, although they accurately determined the location of the defects, could not define the shapes of the defects exactly. Bergant et al. [27] placed artificial defects of different diameters on the glass/epoxy sample in their study. Although roughness and damage on the peeling surface were detected, no damage thicker than 0.04 mm could be detected.

The damage analysis of composite materials tested with the ultrasonic test method is mostly carried out by using package programs integrated into the ultrasonic system. Package programs that process all samples with the same algorithm have difficulty in achieving the desired level of success due to the wide variety of components used in composite materials. On the other hand, identifying different materials with similar acoustic impedance values creates another problem. Researchers generally attribute the difficulties experienced in the examination of glass fiber reinforced composites, which are widely used in the field of composites, with ultrasonic tests to the morphological structure of these fibers [16,26,28]. In the literature, there are many studies based on the determination of damages that occurred during both the production process and the use of ultrasonic test methods. These studies generally aim to detect artificial damage in different sizes and structures [29–32]. However, there have been no studies on any damage analysis of the actual damage that would occur as a result of an external impact on an internally damaged material.

The first purpose of this study was to determine the various artificial damages caused to composite materials during the manufacturing process. With these artificial damages, some defects that may be encountered during composite production have been tried to be simulated as defects caused by foreign matter (tape residues, cured epoxy wastes, plastic residues) or woven fabrics used as reinforcement materials during production. Artificially damaged composites were produced using glass and carbon woven fabric, which are widely used in the field of fiber reinforced composites. The second goal was to find out how much load artificially defective areas could withstand and investigate this trend through ultrasonic non-destructive testing and sample-based image processing algorithms. In line with this purpose, different reinforcement materials were utilized in the production of composites, and various types and orientations of damages were detected using the ultrasonic C-scan method. The developed image processing algorithms enhanced the visibility of damages, and the limit as well as the dimensions of damages were calculated. It is believed that this scanning method and the developed algorithms for detecting BVID damages will provide a different perspective in the literature.

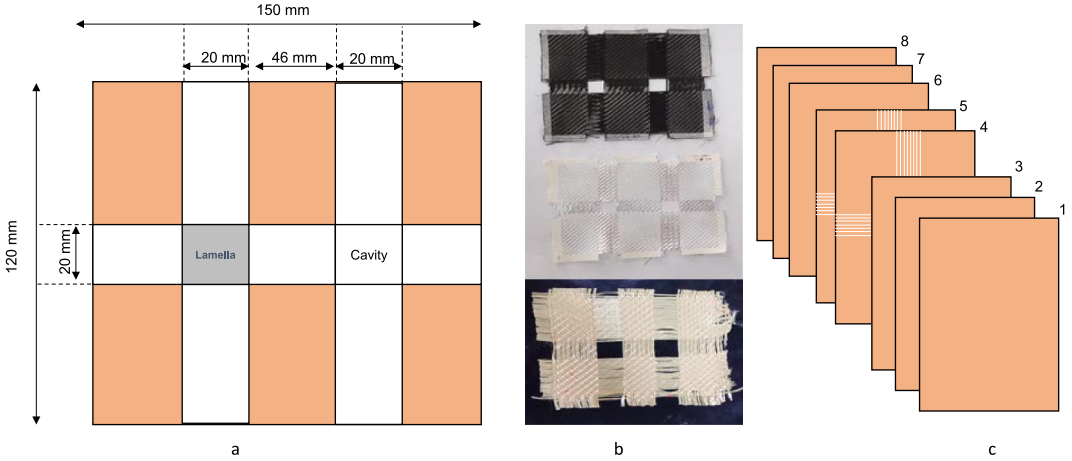

Fig. 1. Artificial damage geometry **(a)**, Artificially damaged layers **(b)**, Placement of artificially damaged layers in the sample **(c)**.

2. Experimental study

2.1. Materials

In the study, composite samples were manufactured from woven glass and carbon materials with $[0^{\circ}]_8$ configurations with 280 and 245 g/m^2 areal densities, respectively. Each sample, consisting of 8 layers of fabric with dimensions of 150 mm × 120 mm was infused with L160 epoxy resin and H160 hardener (Hexion MGS) using a vacuum bagging method at 80 °C for 1 h.

2.2. Geometry of artificial damage

First, 14 filaments were drawn from the glass and carbon reinforcement fabrics in both warp and weft directions in 2 consecutive layers of each sample. In this way, two spaces of 20 mm × 20 mm were created at the intersection of the weft and warp filaments shown in Fig. 1a and b. These 2 fabrics were placed in the middle of the composite structure located on the 4th and 5th layers as shown in Fig. 1c.

Then, in one of the cavities of the 4th and 5th layers, two pieces of glass lamella were placed on top of each other, while the other cavity was left empty. Thus, during the casting of epoxy resin by vacuum bagging, two different artificial damage were created, one of which was filled with glass lamella, and the other cavity was filled with epoxy resin.

According to the specified experimental plan, carbon and glass fabric layers were prepared on a vacuum infusion table (Fig. 2a). Samples were impregnated with resin using the VARTM method (Fig. 2b). After the resin transfer, the samples were cured at 80 °C for 2 h, resulting in the production of damaged and undamaged specimens (Fig. 2c and d). The thickness of GFRP and CFRP were 2.913 and 2.553 mm, respectively.

2.3. Ultrasonic inspection

These samples were subjected to a series of ultrasonic tests to detect artificial damage by applying the ultrasonic TTU method in an immersion-type US 100 ultrasonic test device. In so-called immersion systems, the sample is examined in a water tank to remove air between the sample and two probes positioned in the same plane with each other to obtain convenient sound energy levels in the material. One of these probes acts as a transmitter and the other as a receiver, showing great success in detecting discontinuities even when the signal strength is weak [33]. The US100 device used in this study, developed by Ultrasonar in 2018, has a computer-controlled automatic dipping system (Fig. 3).

The samples placed in the immersion-type ultrasonic test device with 3 MHz frequency probes were examined. The first raw images in gray image format obtained from the interface were then rearranged with image processing algorithms.

2.4. Drop-weight impact test

The drop-weight impact test was applied to the samples to investigate the impact behavior of the internally damaged samples. Before testing, the inner structure of each sample was examined with an ultrasonic test device. The impact properties of composite samples were tested with the BESMAK drop weight impact tester at Istanbul Technical University Composite Laboratory. Three samples were taken from each composite AL, AC, and UD as a reference sample. The samples were prepared according to the device standards with the dimensions of 55 mm × 89 mm. Then a 16 mm diameter drop-weight striking head was positioned to target the center of the damaged area, and 20 J energy was applied.

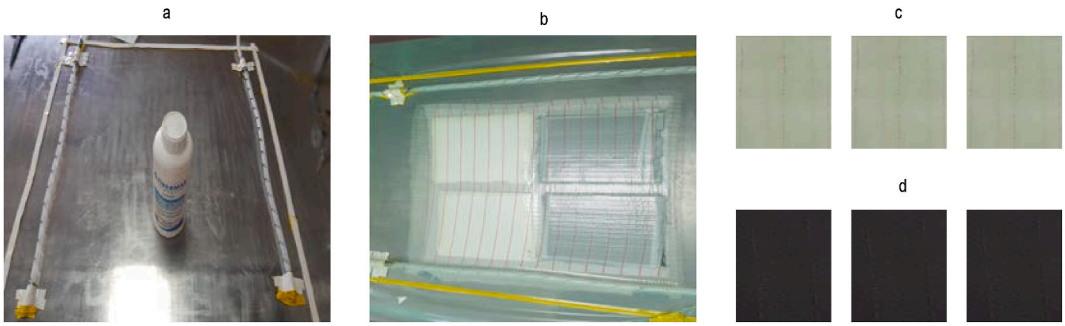

Fig. 2. Composite production according to the VARTM method.

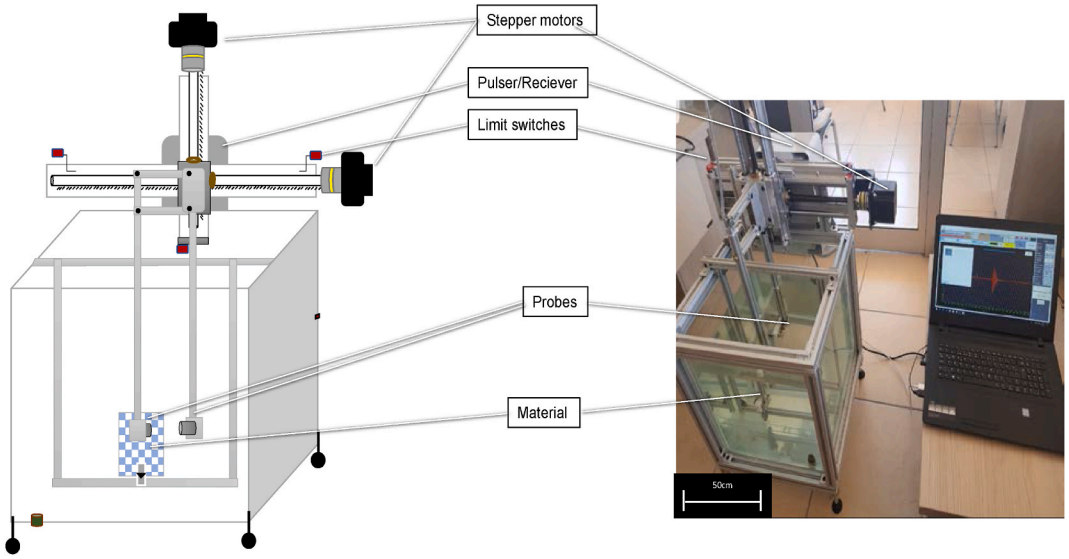

Fig. 3. US100 Ultrasonic non-destructive testing device.

3. Result and discussion

3.1. Ultrasonic test results

Before conducting the drop-weight impact test, a series of ultrasonic tests were performed to determine the location and dimension of the artificial damage in the samples produced. As seen in Fig. 4, embedded damages in the samples were detected with a US 100 ultrasonic testing device, and the first grayscale data were obtained. The image of the glass fabric reinforced composite was more dispersed and not clearer than the CFRP. The reason for this may be more scattering of ultrasonic sound signals sent to the sample in the amorphous structure of the glass fiber. In both samples, it was very difficult to detect epoxy-filled artificial defect areas, even with ultrasonic inspection.

3.2. Image processing algorithm

The artificial damage found in the first images we obtained with grayscale from the ultrasonic imaging tester was very difficult to detect (Fig. 4a and b). For this reason, image processing algorithms were developed with the MATLAB package program to make an image of damage clearer. After determining the damage shape inside the composite, the damaged area could be calculated.

As followed in Fig. 5, in the first place (Fig. 5a), noise-removing filters are applied to the gray image to eliminate the noises that come from the image acquisition process. Thus, a cleaner image frame was obtained to be used for the kernel. “Gaussian Filter” applied

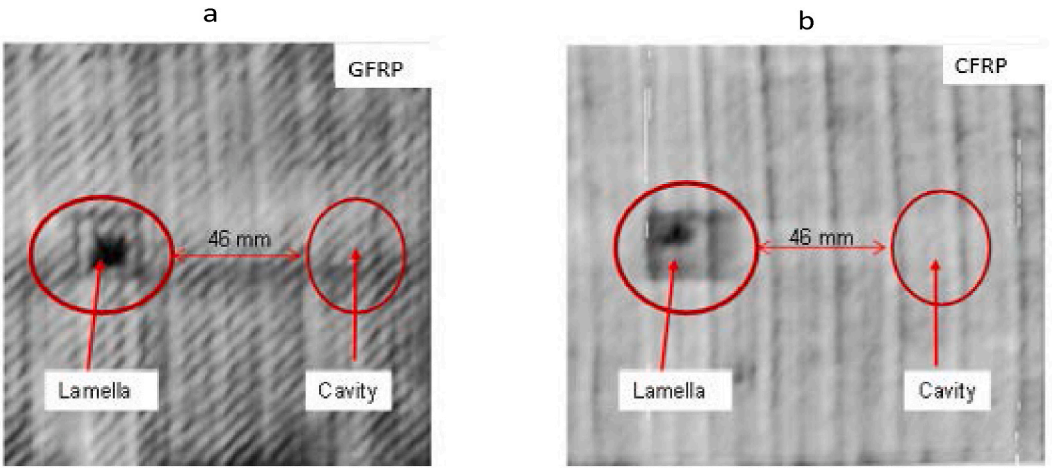

Fig. 4. Gray-scaled images of GFRP**(a)** and CFRP**(b)** containing artificial damages from US 100 ultrasonic testing device.

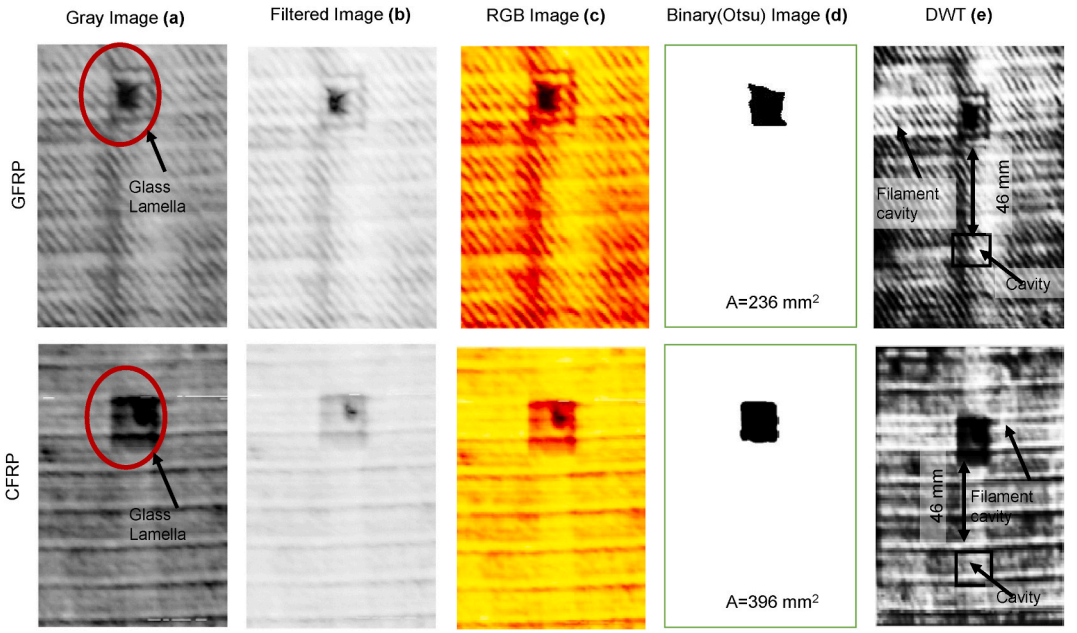

Fig. 5. The First image: is taken as a gray image **(a)**, the second image is Median Gaussian filtered **(b)**, the third image: is converted to RGB color space with a Hot map **(c)**, the fourth image is a binary image with the Otsu method **(d)**, the fifth image is a processed with DWT db5 wavelet **(e)**.

to soften the image frame thereby weakening and blurring the background texture (Fig. 5b). Then RGB (Fig. 5c) and Otsu (Binary) (Fig. 5d) methods were used to improve the filtered images followed by Discrete Wavelet Transform methods (Fig. 5e).

Discrete Wavelet Transform (DWT) was used to decompose the image into four sub-images; approximation images (Fig. 6a) and

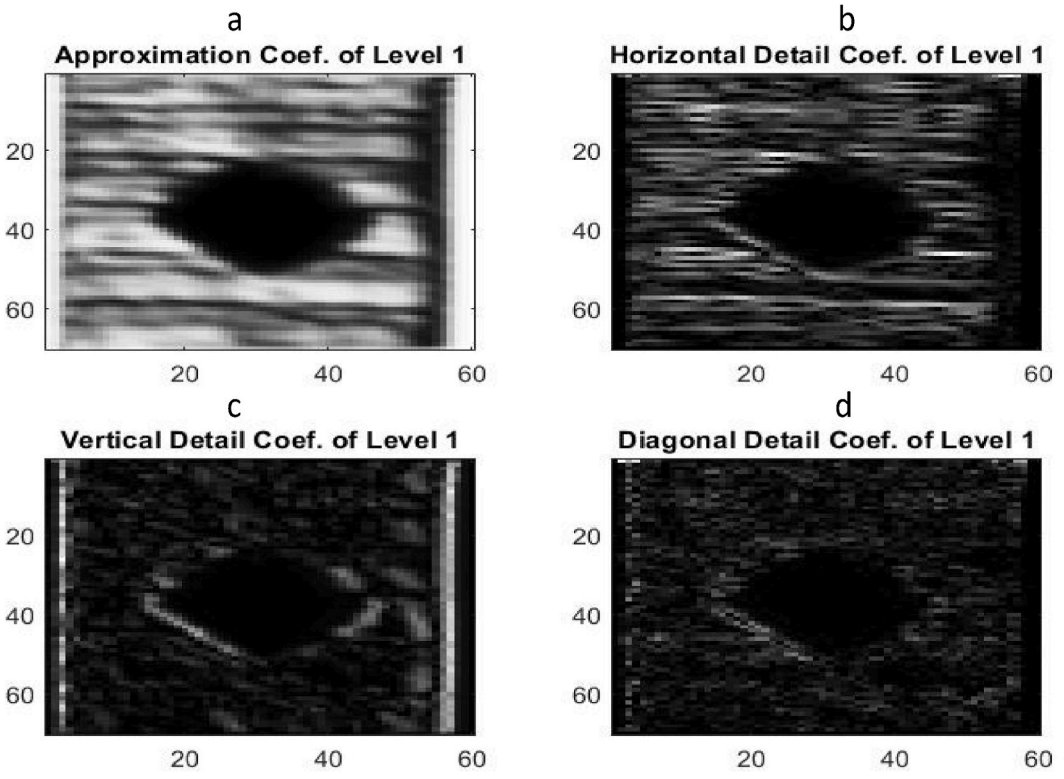

Fig. 6. C/UD sample image processing by DWT method, approximation images **(a)**, horizontal detail **(b),** vertical detail **(c)**, diagonal detail **(d)**.

detail images horizontal (Fig. 6b), vertical (Fig. 6c), and diagonal details (Fig. 6d) at one resolution level by using a 'db5' type wavelet. MATLAB program includes several families of wavelet that have proved to be useful for different types of applications. Since tailoring the choice of best wavelet depends on the image size and desired quality reconstructed image [34–36], in this study some pre-determined mother wavelets such as Haar, Daubechies, Symlets, Coiflets, and biorthogonal were applied to image frames and compared in terms of their defect segmentation. According to the visual comparison, it was revealed that the highest segmentation result was obtained with 'Daubechies'. In the MATLAB program, the names of the Daubechies family wavelets are written dbN, where N is the order, and db is the "surname" of the wavelet. There are nine members of Daubechies from "db2" to "db10". The best choice of the mother wavelet was determined as "db5" among nine alternatives by trial and error.

This newly developed image analysis algorithm method named Ozce was applied to the samples before and after the weight drop impact test and helped to reveal their damage behavior. Although the acoustic impedance values of glass fabric and glass lamella were close to each other, the algorithm was able to distinguish these two structures very easily. However, images from the artificial cavity filled with epoxy defects were not as clear as glass defects. The number of black pixels in the binary image that corresponds to the damage was counted and multiplied by pixel size. Thus, the value of the damaged area was calculated in square millimeters (Fig. 5d). The damaged area was calculated as 396 mm^2 in the CFRP, which was very close to the original area of 400 mm^2. As can be seen from the first three images, the epoxy resin penetrated inward from the edges of the two thin glass lamellas placed on top of each other but did not completely cover the inner surface. This led to the formation of an air gap in the center of the lamella layers. The calculated GFRP damage area due to epoxy seeping from the edges caused the artificial damage area to be smaller than the original CFRP area. As a result, the artificial damage area with glass lamella calculated in the GFRP was calculated as 236 mm^2.

3.3. Drop weight impact test

The drop weight impact test results performed on artificially damaged and undamaged samples are given in Table 1.

Peak force values of GFRP composites in all three forms (G/UD, G/AC, G/AL) were higher than samples (C/UD, C/AC, C/AL) (Fig. 7a and b). The maximum strength value that the artificially damaged specimens could bear decreased between 20.25% and 33.29%, as expected, compared to the undamaged specimens. As shown in Fig. 6, the maximum deformation (mm) value increased in artificially damaged composite structures in both GFRP and CFRP composites compared to undamaged GFRP and CFRP composites. The highest deformation value was measured as 8.624 mm in the GFRP composites G/AL, while 12.412 mm in the CFRP composites C/AL inserted. For GFRP, displacement values increased up to 38% in G/AL, while this value was 29% in G/AC. Since the striking head at the drop-weight test could not fully penetrate some samples, some of the impact energy was stored as elastic energy, causing the striking head to bounce back. The highest elastic recovery was calculated as 32% for G/UD, followed by 28% for G/AC and 26% for G/AL. On the other hand, only C/UD showed 19% elastic recovery, and the other CFRP with the artificially damaged punctured under an impact force.

According to the energy-time graph of damaged and undamaged forms of GFRP composites with applied 20 J energy, the energy absorption values were closer to each other than CFRP composites (Fig. 8a and b). All samples absorbed 67%–88% of the 20 J energy, C/UD having the highest energy absorption of 17.507 J (Fig. 8b). The measured deformation time for G/UD was less than for both artificially damaged samples (Fig. 8a). In contrast, deformation times were higher in artificially damaged CFRP composites than in C/UD.

When the literature is examined, most of the studies have been carried out to determine the artificial damages placed on composite structures or the capabilities of different measurement methods. However, since there are not many studies on the effect of internal defects on actual damage, it was aimed to investigate this phenomenon by examining it with a newly developed image-analyzing algorithm called Ozce.

In addition, an important problem encountered in GFRP in these studies, due to the morphological structure of glass fiber, is the inability to determine the direction and boundaries of damage. In our study, we tried to minimize this disadvantage by using an Ozce algorithm. With the developed image processing algorithm, the damaged areas formed after the drop weight impact test were calculated on the samples. Damaged area values in GFRP were calculated as 72.88 mm^2 in the G/UD sample, 143.74 mm^2 in the G/AC sample, and 315.93 mm^2 in the G/AL sample (Fig. 9c). In CFRP, it was calculated as 303.86 mm^2 in the C/UD sample, 356.52 mm^2 in the C/AC sample, and 385.95 mm^2 in the C/AL sample (Fig. 9g). The fact that the damaged area values are close to each other in CFRP is thought to be caused by the perforation of the artificially damaged samples and therefore stopping the progression of the damaged

Table 1
Impact test results of composites.

Impact energy	Sample	Peak Force (N)	Maximum deformation (mm)	Absorbed energy (J)	Elastic Recovery (%)	Damaged area* (mm^2)
20J	G/UD	4675	6.231	16.779	%32	72.88
	G/AC	3225	8.055	16.869	%28	143.74
	G/AL	3354	8.624	17.059	%26	315.93
20J	C/UD	3136	7.940	17.507	%19	303.86
	C/AC	2501	11.811	15.514	–	356.52
	C/AL	2092	12.412	13.352	–	385.95

G: GFRP, C: CFRP, UD: undamaged, AC: artificially damaged with epoxy-filled, AL: artificially damaged with glass lamella, * Evaluated from C-Scan images.

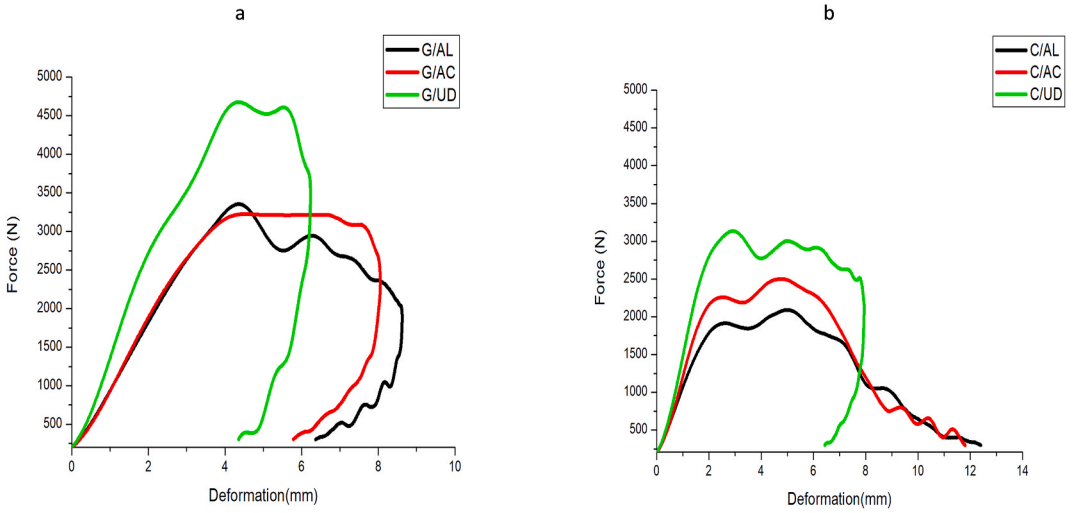

Fig. 7. Force-deformation graphics of GFRP **(a)** and CFRP **(b).**

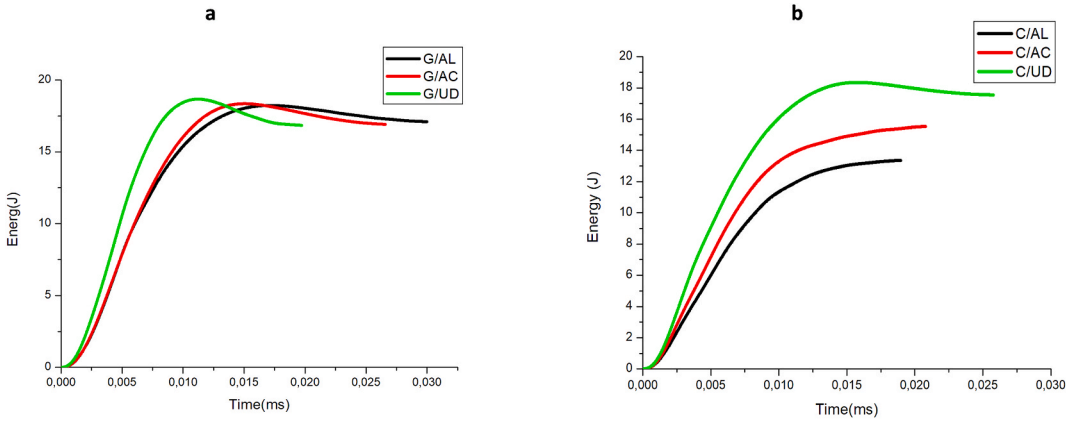

Fig. 8. Energy-time history of GFRP **(a)** and CFRP **(b).**

area (Fig. 9h). Glass and carbon composites show different damage behaviors under load due to their different morphological structures. Another factor affecting damage behavior is reinforcement fabric properties such as weft density, warp density, and fabric weight [37]. The thickness of the composite produced and the fiber volume ratio are other important factors. While glass composites are under load, the load transferred to the sample is more spread out, while in carbon composites the load may cause more local breakage.

It is thought that the reason why samples with artificial damage containing glass lamella undergo further deformation was that the air between the two lamella was compressed with the impact received and this glass lamella in the composite might be broken down into smaller glass particles and scattered around, causing greater damage to the surrounding area. As a result, damaged fibers showed lower resistance against impact as reinforcement material.

CFRP and GFRP were artificially damaged during composite manufacturing and then exposed to impact load. In GFRP, the damage area in the G/AL was calculated 4–5 times more than in the G/UD. If perforation occurred, the damage area values remained constant at a certain point in CFRP samples. While perforation did not occur in the C/UD, perforation occurred in both CFRPs with artificial damage. This is an example of the damage that such artificial damages would cause in the future if left undetected.

When the damaged areas were examined in CFRP and GFRP after the drop weight impact test, the artificial damages created with the cavity structure gave better results than the artificial damages created with the glass lamella. The main reason for this may be that the addition of glass lamella may cause a shearing effect that increases the deformation area in the fibers due to breakage due to the impact effect, and thus catastrophic fiber and matrix fractures occur in composites [38]. In addition, the addition of glass lamella can increase the stiffness of the composite structure and make the structure more brittle under impact load.

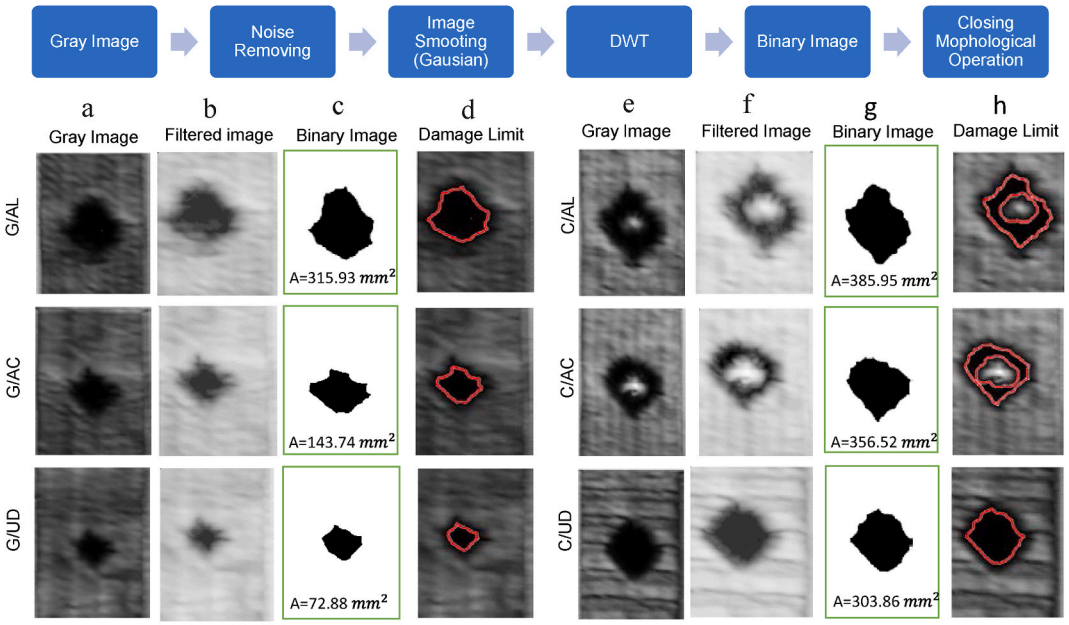

Fig. 9. Application of image processing algorithms to the samples.

4. Conclusions

This study aims to detect damages that are usually not possible to detect visually, before and after impact, by ultrasonic non-destructive testing method. At the same time, the importance of damage detection was emphasized with the weight drop impact tests performed. The dimensions of the damaged areas vary significantly in the tests conducted on artificially damaged and undamaged samples. The damage that occurred after the impact test in the G/AL sample, produced with the same parameters, was approximately five times greater than that in the G/UD sample. Furthermore, while the C/UD sample did not experience perforation after the impact test, both the C/AL and C/AC samples were perforated.

Detection of damages before and after the impact test was carried out using ultrasonic scanning data and developed image processing algorithms. To better understand the sensitivity of the developed algorithm, glass lamellas were used as artificial damage, especially in glass fiber-reinforced samples. In addition, detecting the cavity structure, which is another type of artificial damage in the sample, is an extremely challenging process.

With the developed image processing algorithms, the orientation, limits, and area calculations of the damages were done successfully. In particular, the effectiveness of the DWT (Discrete Wavelet Transform) method for the detection of cavity and lamella structures has come to the fore.

As a result, considering the studies carried out, it is important to detect the errors that occur during the composite production stage before use, in terms of the bad consequences they will cause. Such damages can be successfully detected with ultrasonic non-destructive testing methods and image processing algorithms.

CRediT authorship contribution statement

Burak Öztaş: Writing – review & editing, Writing – original draft, Visualization, Software, Resources, Project administration, Formal analysis, Data curation, Conceptualization. **Yasemin Korkmaz:** Supervision, Project administration, Methodology, Investigation, Funding acquisition, Conceptualization. **Halil İbrahim Çelik:** Writing – review & editing, Visualization, Validation, Software, Formal analysis, Data curation.

Declaration of competing interest

The authors declare the following financial interests/personal relationships which may be considered as potential competing interests:Burak OZTAS reports financial support was provided by Kahramanmaras Sutcu Imam University. Burak oztas reports a relationship with Kahramanmaras Sutcu Imam University that includes: employment.

Acknowledgements

This study was supported by Kahramanmaras Sutcu Imam University- BAP and DOSAP coordination unit within the scope of project no 2018/4–14 D and 2022/5–19. The authors acknowledge Gaye KAYA and Erdem SELVER for their contributions during the research.

References

[1] H. Ahmad, A.A. Markina, M.V. Porotnikov, et al., Review of carbon fiber materials in the automotive industry, IOP Conf. Ser. Mater. Sci. Eng. 971 (2020), https://doi.org/10.1088/1757-899X/971/3/032011.
[2] T.P. Sathishkumar, J. de-Prado-Gil, R. Martínez-García, et al., Redeemable environmental damage by recycling of industrial discarded and virgin glass fiber mats in hybrid composites—an exploratory investigation, Polym. Compos. 44 (1) (2023) 318–329, https://doi.org/10.1002/pc.27047.
[3] S. Kumar, A. Bhandari, R. Sharma, et al., Polymer matrix composites: a state of art review, Mater. Today Proc. 57 (2022) 2330–2333, https://doi.org/10.1016/j.matpr.2021.12.592.
[4] K. Friedrich, A.A. Almajid, Manufacturing aspects of advanced polymer composites for automotive applications, Appl. Compos. Mater. 20 (2013), 107–128.10.1007/s10443-012-9258-7.
[5] H.L. Ma, Z. Jia, K.T. Lau, et al., Impact properties of glass fiber/epoxy composites at cryogenic environment, Compos. Part B Eng. 92 (7) (2016) 210–217, https://doi.org/10.1016/j.compositesb.2016.02.013.
[6] A. Maziz, M. Tarfaoui, L. Gemi, et al., A progressive damage model for pressurized filament-wound hybrid composite pipe under low-velocity impact, Compos. Struct. 276 (2021) 114520, https://doi.org/10.1016/j.compstruct.2021.114520.
[7] T. Jollivet, C. Peyrac, F. Lefebvre, Damage of composite materials, Procedia Eng. 66 (2013) 746–758, https://doi.org/10.1016/j.proeng.2013.12.128.
[8] A.S. AlOmari, K.S. Al-Athel, A.F.M. Arif, et al., Experimental and computational analysis of low-velocity impact on carbon-, glass-and mixed-fiber composite plates, Journal of Composites Science 4 (4) (2020) 148, https://doi.org/10.3390/jcs4040148.
[9] A. Katunin, A. Wronkowicz-Katunin, K. Dragan, Impact damage evaluation in composite structures based on the fusion of results of ultrasonic testing and x-ray computed tomography, Sensors 20 (2020) 1867, https://doi.org/10.3390/s20071867.
[10] A. Sellitto, A. Riccio, A. Russo, et al., Ultrasonic damage detection of impacted long and short fibre composite specimens, Key Eng. Mater. 827 (2020) 31–36, https://doi.org/10.4028/www.scientific.net/KEM.827.31.
[11] C. Ibarra-Castanedo, P. Servais, M. Klein, et al., Detection and Characterization of Artificial Porosity and Impact Damage in Aerospace Carbon Fiber Composites by Pulsed and Line Scan Thermography, Applied Sciences 13 (10) (2023) 6135. https://doi.org/10.3390/app13106135.
[12] H. Cao, M. Ma, M. Jiang, et al., Experimental investigation of impactor diameter effect on low-velocity impact response of CFRP laminates in a drop-weight impact event, Materials 13 (2020) 4131, https://doi.org/10.3390/ma13184131.
[13] I. Dafydd, Z. Sharif Khodaei, Analysis of barely visible impact damage severity with ultrasonic guided Lamb waves, Struct. Heal. Monit. 19 (2020) 1104–1122, https://doi.org/10.1177/14759217198788.
[14] S.Z.H. Shah, S. Karuppanan, P.S.M. Megat-Yusoff, et al., Impact resistance and damage tolerance of fiber reinforced composites: a review, Compos. Struct. 217 (2019) 100–121, https://doi.org/10.1016/j.compstruct.2019.03.021.
[15] C. Garnier, M.L. Pastor, F. Eyma, et al., The detection of aeronautical defects in situ on composite structures using Non Destructive Testing, Compos. Struct. 93 (5) (2011) 1328–1336, https://doi.org/10.1016/j.compstruct.2010.10.017.
[16] T. Hasiotis, E. Badogiannis, N.G. Tsouvalis, Application of ultrasonic C-scan techniques for tracing defects in laminated composite materials, Stroj. Vestnik/Journal Mech. Eng. 57 (2011) 192–203, https://doi.org/10.5545/sv-jme.2010.170.
[17] I. Papa, V. Lopresto, G. Simeoli, A. Langella, et al., Ultrasonic damage investigation on woven jute/poly (lactic acid) composites subjected to low velocity impact, Compos. Part B Eng. 115 (2017) 282–288, https://doi.org/10.1016/j.compositesb.2016.09.076.
[18] F. Pinto, L. Boccarusso, D. De Fazio, et al., Carbon/hemp bio-hybrid composites: effects of the stacking sequence on flexural, damping and impact properties, Compos. Struct. 242 (2020) 112148, https://doi.org/10.1016/j.compstruct.2020.112148.
[19] E. Selver, B. Öztaş, M. Uçar, Mechanical and thermal properties of glass/epoxy composites filled with silica aerogels, Plast., Rubber Compos. 50 (2021) 371–383, https://doi.org/10.1080/14658011.2021.1903142.
[20] G. Kaya, Comparison of the impact damage resistance of non-hybrid and intra-ply hybrid carbon/E-glass/polypropylene non-crimp thermoplastic composites, J. Reinf. Plast. Compos. 38 (2019) 31–45, https://doi.org/10.1177/0731684418805561.
[21] I. Infanta Mary Priya, B.K. Vinayagam, Detection of damages on biaxial GFRP composite material using non-destructive technique, Polym. Bull. 78 (2021) 2569–2603, https://doi.org/10.1007/s00289-020-03228-x.
[22] V. Kostopoulos, A. Kotrotsos, A. Geitona, et al., Low velocity impact response and post impact assessment of carbon fiber/epoxy composites modified with Diels-Alder based healing agent, A novel approach. Composites Part A: Applied Science and Manufacturing 140 (2021) 106151, https://doi.org/10.1016/j.compositesa.2020.106151.
[23] P. Jakubczak, J. Bienias, Non-destructive damage detection in fibre metal laminates, J. Nondestr. Eval. 38 (2) (2019) 49, https://doi.org/10.1007/s10921-019-0588-3.
[24] A. Vyas, S. Yu, J. Paik, Fundamentals of digital image processing, Signals Commun. Technol. (2018) 3–11, https://doi.org/10.1007/978-981-10-7272-7_1.
[25] A. McAndrew, An Introduction to Digital Image Processing with Matlab Notes for SCM2511 Image Processing 1 Semester 1, School of Computer Science and Mathematics, Victoria University of Technology, 2004, pp. 1–264.
[26] A.A. Hassen, H. Taheri, U.K. Vaidya, Non-destructive investigation of thermoplastic reinforced composites, Compos. Part B Eng. 97 (2016) 244–254, https://doi.org/10.1016/j.compositesb.2016.05.006.
[27] Z. Bergant, J. Janez, J. Grum, Ultrasonic c-scan testing of epoxy/glass fiber composite, in: Application of Contemporary Non-destructive Testing in Engineering, 2017, pp. 41–48.
[28] J. Dong, B. Kim, A. Locquet, et al., Nondestructive evaluation of forced delamination in glass fiber-reinforced composites by terahertz and ultrasonic waves, Compos. Part B Eng. 79 (2015) 667–675, https://doi.org/10.1016/j.compositesb.2015.05.028.
[29] W. Post, M. Kersemans, I. Solodov, et al., Non-destructive monitoring of delamination healing of a CFRP composite with a thermoplastic ionomer interlayer, Compos. Part A Appl. Sci. Manuf. 101 (2017) 243–253, https://doi.org/10.1016/j.compositesa.2017.06.018.
[30] A. Katunin, K. Dragan, M. Dziendzikowski, Damage identification in aircraft composite structures: a case study using various non-destructive testing techniques, Compos. Struct. 127 (2015), https://doi.org/10.1016/j.compstruct.2015.02.080, 1–9.
[31] I. Papa, M.R. Ricciardi, V. Antonucci, et al., Comparison between different non-destructive techniques methods to detect and characterize impact damage on composite laminates, J. Compos. Mater. 54 (2020) 617–631, https://doi.org/10.1177/0021998319864411.
[32] H. Taheri, A.A. Hassen, Nondestructive ultrasonic inspection of composite materials: a comparative advantage of phased array ultrasonic, Appl. Sci. 9 (2019) 1628, https://doi.org/10.3390/app9081628.
[33] K. Yadav, R. Kumar, N. Dhiman, et al., Development and study of ultrasonic immersion testing system for industrial and metrological application, J. Instrum. 18 (2023), https://doi.org/10.1088/1748-0221/18/03/P03001.
[34] G.K. Kharate, V.H. Patil, N.L. Bhale, Selection of mother wavelet for image compression on basis of nature of image, J. Multimed. 2 (2007) 44–51, https://doi.org/10.1109/ICSCN.2007.350747.
[35] S. Sridhar, P. Rajesh Kumar, K.V. Ramanaiah, Wavelet Transform techniques for image compression – an evaluation, Int. J. Image Graph. Signal Process. 6 (2014) 54–67, https://doi.org/10.5815/ijigsp.2014.02.07.

[36] R. Thakur, R. Gupta, S. Shukla, Selection of wavelet from wavelet families to facilitate the evolution of color image denoising, International Journal of advance research, IJOAR. org 1.2 (2013) 217–221.
[37] P. Schwartz (Ed.), Structure and Mechanics of Textile Fibre Assemblies, Woodhead publishing, 2019, 9780081026199.
[38] Y. Gaye, Experimentally Determination of the Mechanical Properties of Stitched and Containing Nano-Particle Multilayered E-Glass/polyester Woven Fabric Composites Erciyes Üniversitesi, 2013, pp. 42–44.